Article

Thermal and Flammability Characteristics of Blended Jatropha Bio-Epoxy as Matrix in Carbon Fiber–Reinforced Polymer

Mohd Radzi Mohd Hafiezal [1,2,]*[ ]**, Abdan Khalina** [1,3,]***, Zainal Abidin Zurina** [1,4]**,
Md Deros Mohd Azaman** [5] **and Zin Mohd Hanafee** [6]

[1] Department of Biological and Agricultural Engineering, Faculty of Engineering, Universiti Putra Malaysia, Serdang 43400, Malaysia; zurina@upm.edu.my
[2] Faculty of Engineering Technology, Universiti Malaysia Perlis, Perlis 02100, Malaysia
[3] Institute of Tropical Forestry and Forest Products (INTROP), Universiti Putra Malaysia, Serdang 43400, Malaysia
[4] Department of Chemical and Environmental Engineering, Faculty of Engineering, Universiti Putra Malaysia, Serdang 43400, Malaysia
[5] School of Manufacturing Engineering, Universiti Malaysia Perlis, Perlis 02600, Malaysia; azaman@unimap.edu.my
[6] Aerospace Malaysian Innovative Centre, No. 3-6-01, GMI, Kajang 43000, Malaysia; hanafee@amic.my
* Correspondence: hafiezalradzi@gmail.com (M.R.M.H.); khalina@upm.edu.my (A.K.);
Tel.: +60-13-625-7374 (M.R.M.H.); +60-16-311-1711 (A.K.)

check for updates

Abstract: This purpose of this paper was to reveal characteristics of a composite structure containing carbon fiber as a reinforcement and blended synthetic epoxy/bio-epoxy derived from crude jatropha oil as resin and compared with fully synthetic epoxy. The composite structure was prepared by the vacuum-assisted resin transfer molding technique and was left to cure for 24 h at room temperature. Both were characterized for their thermal, chemical, and flammable characteristics. The incorporation of jatropha bio-epoxy into the matrix significantly improved the thermal stability between 288–365 °C as obtained by thermogravimetric analysis (TGA) test. Dynamic mechanical analysis (DMA) curves showed slight diminution of performances and T_g from DMA tests confirmed well with the trend of T_g obtain by differential scanning calorimetry (DSC) curves. On the other hand, the flammability property was rated horizontal burning (HB) which was the same as the fully synthetic composite, but the duration to self-extinguish was halved for the composite with jatropha bio-epoxy. Fourier transform infrared attenuated total reflectance (FT-IR/ATR) was conducted to determine the difference of functional groups' spectrum due to bonding type existing on both specimens. Overall, the composite specimen with blended bio-epoxy exhibited better thermal stability, comparable flammability characteristics, and performances. The aim of this paper was to introduce bio-based epoxy as a potential alternative epoxy and to compete with synthetic epoxy so as to minimize the footprint of non-renewable composite.

Keywords: jatropha bio-epoxy; bio-composite; thermal; flammability; bio-matrix

1. Introduction

Composite material is very common in the transportation industry and construction sector. Most composite materials contain epoxy as its matrix binds the reinforcement, as the loading is distributed amongst the fibers inside it. Around 60% of global epoxy is used in coating applications, and around 40% in adhesive and assembly applications [1]. This large amount of usage leaves

significant environmental post-usage footprints, in addition to the unstable price factor of petroleum as its main source, which are the main drawbacks of epoxy.

Jatropha plant is unpopular due to being inedible. The plant can be found in most forests in Malaysia, and recently its oil was developed to become bio-fuel in machineries, trucks, and jet engines [2]. Previous research has been carried out on their physical and mechanical performances and they showed good and reliable results [3,4].

Recent studies on epoxidized jatropha oil by researchers around the world have shown its superiority of chemical resistance compared to a palm-oil-based adhesive when used as a wood adhesive [5]. Sammaiah et al. [6] reported that a comparison between epoxidized jatropha oil with epoxidized soybean oil (ESBO) for lubrication application is comparable in terms of oxidative stability, since the epoxidized jatropha oil has a very high reaction conversion of epoxidation of up to 92%. Another study concluded that jatropha oil has good potential as a technical oil, for example, in bio-carburant, soaps, painting, lubricants, and insecticides. This is because jatropha oil contains a high level of unsaturated acid, a high level of crude protein, and a low water-solubility content [7].

The use of bio-epoxy is becoming more popular, but only a limited amount of significant research has been performed to study and develop it. The main bio-epoxy resources are vegetable oils. Niedermann et al. tried sugar-based epoxy resin in jute and a carbon fiber reinforcement. It was found that bio-epoxy had a high glass transition temperature, T_g (160 °C) and its tensile and flexural performances were comparable to synthetic epoxy. It was cured with an amine type curing agent permitted in aerospace applications [8]. Szolnoki et al. reported that a sugar-based component (sorbitol polyglycidyl ether, SPE) was used as an epoxy with a phosphorus content of 1–5% in order to increase its flammability performance, and they successfully reduced its mass loss rate during burning and reached the self-extinguished rate [9].

In another study, Adlina et al. epoxidized sucrose soyate (ESS) from sucrose and soybean oil and cured it with cycloaliphatic anhydride without reinforcement. It was found that its performances could be attributed to the crosslink density and polymer backbone due to the inter and intra-molecular linkage of ESS molecules, polyetherification, entanglement, actual crosslink molecule networks, and dangling from the unreacted functional group [2]. Kunwei et al. produced a bio-renewable thermoset based on acrylated epoxidized soybean oil and methacrylatedeugenol and tested its characteristics. It was found that it possessed high strength and modulus, was thermally stable up to 300 °C, and had a good gelation time which cured within 10 min [10].

It can be concluded that several studies and experiments have been carried out on epoxidized jatropha oil for use in many applications such as coatings, adhesives, tribology, and polymers [11,12]. However, research about epoxidized jatropha oil for composite applications, especially for aerospace products is scarce, thus this paper could increase the potential use of jatropha oil in this sector.

Some vegetable oils have also been epoxidized such as soybean, karanja oil, kraft lignin, sucrose soyate, and palm oil [2,11–13]. Still, they were not used with fiber reinforcement. Most of the results of the characterization have shown good thermal stability, good chemical reaction, and acceptable mechanical properties even though synthetic epoxy is clearly the best in terms of performance. Many reports have said that despite the good or acceptable characteristics and performance of epoxidized vegetable oil, it is renewable and produced from natural resources, which overall is better in the long term. Some of the epoxidized vegetable oils are mixed with some additives in order to obtain better characteristics dependent on the application. It could be said that there is no limit on how we could use and modify these renewable bio-epoxies for different applications. Researchers have found many interesting methods and processes for obtaining good bio-epoxy. As for composite application in the aerospace sector, it is crucial that the bio-epoxy is thoroughly tested and characterized with good consistency of results. This is important because natural resource products behave differently dependent on the batches of cultivation, the environment, and the conditions during cultivation.

2. Materials and Methods

2.1. Fabrication and Materials of the Composite Specimen

Two composite panels were fabricated in this experiment. The first one was made using a fully synthetic epoxy and the second one was made using a synthetic epoxy resin blended with 18 wt.% jatropha bio-epoxy by weight percentage. The synthetic epoxy brand was Epoximite 100 with slow hardener 103 with an instruction ratio of 28:1. Ten (10) layers of 2 × 2 twill weave carbon fiber (3K 200 gsm) were used for each panel. The carbon fibers and the synthetic epoxy were supplied by Mechasolve Engineering, Selangor, Malaysia, and the jatropha bio-epoxy was supplied by a team composed of the collaboration of the Faculty of Engineering, University Putra Malaysia (UPM) with the Aerospace Malaysian Innovative Centre (AMIC), Kajang, Selangor, Malaysia.

The dimensions of the composite panel structure fabricated by VARTM were 300 mm × 300 mm × 2 mm (width × length × thickness). The fully synthetic composite panel was the control specimen, while the composite panel structure with blended 18 wt.% jatropha bio-epoxy was the evaluated specimen.

A flat mold was used as the base surface for fabricating the composite panel. A release agent was applied onto the surface of the flat mold for easy release. Next, 10 layers of carbon fiber were stacked and arranged. Then a peel ply, a media distributor, an enkafusion mat, and plastic bagging were organized in order, with one inlet for the resin and one outlet for the vacuum. All these materials were secured by the sealant tape surrounding them to trap air and prevent the resin from escaping. Once all were settled, the air was sucked out by vacuum pump until it reached around near vacuum condition. Afterwards, an inlet pipe was opened to let the resin infuse through the carbon fibers, the media distributor, etc. The inlet pipe was closed once almost all the resin had been wetted. The setup was cured at room temperature for 24 h before the vacuum pump was shut off then the composite panel was retrieved from the setup. This similar setup also was used in previous studies [3,4].

2.2. Jatropha Bio-Epoxy Derived from Crude Jatropha Oil

Through the process of the addition, removal, stirring, and washing of the mixture of crude jatropha oil with acids and the amberlite catalyst, bio-epoxy was successfully derived from crude jatropha oil [14]. Table 1 below presents some of the physical properties of crude jatropha oil and jatropha bio-epoxy.

Table 1. Physical properties of jatropha oil and jatropha bio-epoxy.

Physical Property	Crude Jatropha Oil (CJO)	Jatropha Bio-Epoxy	Synthetic Epoxy
Appearance	Liquid (clear yellow color)	Liquid (yellow color)	Liquid (clear color)
Density (g/cm^3)	0.89	1.30	1.10
Dynamic Viscosity at 25 °C (cP)/(Pa·s)	46.80	546.00	650.00
Kinematic Viscosity (mm^2/s)	52.41	588.00	-
Epoxy Equivalent Weight (EEW) (gr/eq)	263.16	328.95	-
Epoxy Value (eq/100 gm)	0.38	0.30	-

2.3. FT-IR/ATR Test

Fourier transform infrared (FT-IR) spectroscopy with attenuation total reflection (ATR) technique was used to detect the presence of functional groups existing in both the fully synthetic and the blended jatropha bio-epoxy in uncured and cured form. The spectra of the material were obtained using an IR spectrometer (Pelkin Elmer Frontier GladiATR, Pike Technology, Madison, WI, USA) scanning over

the surface of the sample in the range of 4000–400 cm^{-1}. Table 2 shows the band of synthetic epoxy, amines, and jatropha bio-epoxy with its corresponding functional group [15–17].

Table 2. FT-IR spectrum of synthetic epoxy and jatropha bio-epoxy.

Resin	Band of Spectrum (cm^{-1})	Functional Group
Synthetic Epoxy	3500	O–H stretching
	3057	Stretching C–H of oxirane ring
	2965–2873	Stretching C-H of CH$_2$ and CH aromatic and aliphatic
	1608	Stretching C=C of aromatic ring
	1509	Stretching C–C of aromatic
	1036	Stretching C–O–C of ethers
	915	Stretching C–O of oxirane group
	831	Stretching C–O–C of oxirane group
	772	Rocking CH$_2$
Amines	3500–3300	N–H
	1650–1500	N–H deformation
Jatropha bio-epoxy	2926–2855	C–H snowboarding vibration (aliphatic carbon)
	1742	C=O stretching frequency of ester
	1462	C–H bending frequency of unsaturated alkene
	1165	C–O stretching frequency of ester
	822	C–O–C oxirane ring
	724	C–H group vibration (aliphatic)

2.4. Thermal Test

2.4.1. Thermal Gravimetric Analysis (TGA)

Thermal gravimetric analysis was conducted according to ASTM E1131 by using TA Instrument Q500 (New Castle, DE, USA) in order to characterize the thermal degradation. The two samples weighed 8.35 mg and 6.38 mg for the fully synthetic composite structure and the blended jatropha bio-epoxy composite structure respectively. They were heated from 30–600 °C with a constant heating rate of 10 °C/min in a nitrogen flow of 50 mL/min.

2.4.2. Differential Scanning Calorimetry (DSC)

Differential scanning calorimetry was conducted according to ASTM D3418 using TA Instrument Q20 to determine the thermal transition characteristics. The two samples weighed 6.06 mg and 5.23 mg for the fully synthetic composite structure and the blended bio-epoxy composite structure respectively. They were heated from 30–300 °C with a constant heating rate of 10 °C/min in a nitrogen flow of 40 mL/min.

2.4.3. Dynamic Mechanical Analysis (DMA)

Dynamic mechanical analysis was conducted according to ASTM D4065 using TA Instrument Q800. Samples of 35 mm × 12 mm for each composite structure were put in single cantilever mode in 30–140 °C with a constant heating rate of 5 °C/min in a nitrogen atmosphere at a frequency of 1 Hz and an amplitude of 15 μm.

2.5. Flammability Test

Three samples with dimensions of 250 mm × 15 mm × 2 mm were used to test the flammability performance according to the horizontal burning UL94 standard test. The samples were mounted horizontally with a stand and burned with a torch at around 1200 °C at a 45° angle of inclination. A flame was ignited at the end of the specimen. This was maintained for 20 s and then it was left to propagate until the flame reached the first mark. If the flame reached the first mark in less than 30 s,

the sample was considered to have failed in the test. Two marks were set on the specimens; the first mark was for the time to start recording, and the second mark was where the flame should stop (75 mm distance from the first mark). The time was recorded until either the flame self-extinguished or the flame reached the second mark.

3. Results and Discussion

3.1. FT-IR Spectrum

Figure 1 shows the FT-IR/ATR comparison data for both the fully synthetic and the blended jatropha bio-epoxy in uncured and cured form. These spectrums were obtained to identify the difference in chemical bonding when jatropha bio-epoxy was added into the matrix.
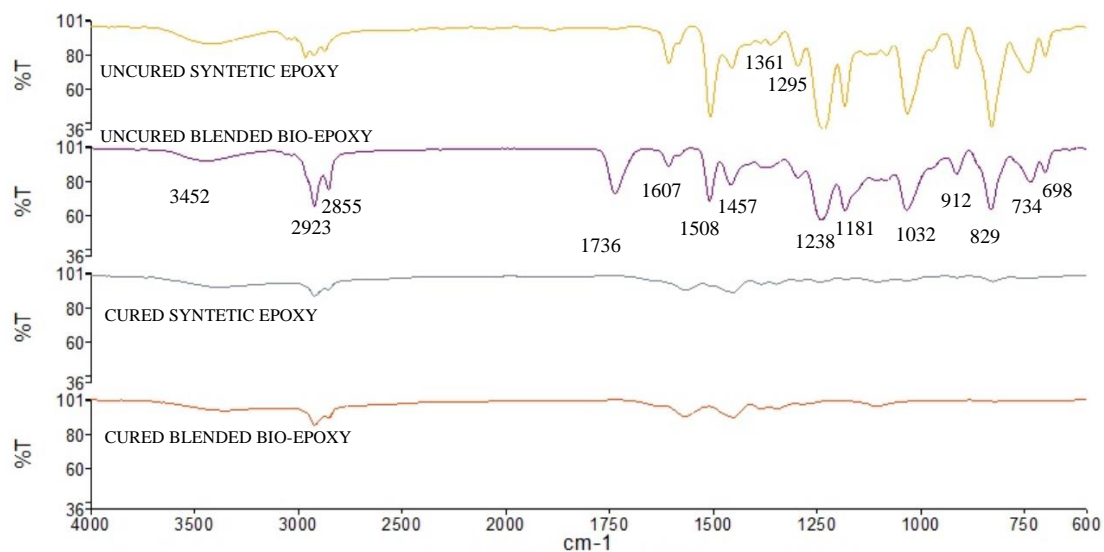
Figure 1. FT-IR/attenuation total reflection (ATR) spectra of the fully synthetic (in uncured and cured form) and the blended bio-epoxy (in uncured and cured form).

The spectrum could be segregated into four regions, spectrum 4000 cm^{-1} to 2500 cm^{-1} which is for N–H, C–H, and O–H single bonds, 2500 cm^{-1} to 2000 cm^{-1} which is for triple bonds, 2000 cm^{-1} to 1500 cm^{-1} which is for C=O, C=N, C=C double bonds, and 1500 cm^{-1} to 400 cm^{-1} is the fingerprint of the compound which are single bonds C–O and double bonds C=C.

In the first region, at band 2923 cm^{-1} and 2853 cm^{-1}, the peak of both bands was sharper, and percentage of transmittance was higher in uncured blended jatropha bio-epoxy compared to others. This is the aliphatic C–H stretching group of alkane compound class and they are commonly found in triglyceride oil [18]. There are no spectrum changes in the second region. Meanwhile, in the third region, a broad and sharp peak at band 1736 cm^{-1} was identified only when jatropha bio-epoxy was added. This was the C=O stretching of ester group which commonly presents in fatty acids [14]. Then in the fourth region, the spectrums became less sharp and a little broader in some of the bands. Essentially at band 829 cm^{-1}, C–O–C stretching of oxyrane group was identified in the blended bio-epoxy as reported in some research papers [11,19,20]. There were O–H bending of phenol group and C–O stretching of aromatic ester at band 1361 cm^{-1} and 1295 cm^{-1}, respectively.

For the cured blended jatropha bio-epoxy, the spectrum was almost identical with the cured synthetic epoxy. This is important as the cross-linking process occurred successfully as the band 829 cm^{-1} disappeared in both cured matrices same as reported by Hazmi et al. [17], Chauhan et al. [21], Tomas et al. [22] and Mincheva et al. [23].

3.2. Thermal Testing Result

3.2.1. Thermal Stability by TGA

The thermograms from TGA can be seen in Figure 2 and the onset temperatures are tabulated in Table 3. The results from the weight loss in the function of temperature increment revealed that there are two thermal degradations. The first degradation occurs at around 100 °C for both the synthetic specimen and the blended jatropha bio-epoxy specimen. This weight loss was due to the evaporation of moisture and other volatile compounds to the environment as heat was applied to the specimen [18]. Both specimens had the same amount of moisture as the first maximum peak of derivative weight loss occurred at 99% at 112 °C for both specimens. The water moisture will act as a plasticizer, reducing the transition glass temperature of a composite structure [24,25]. Besides, those spaces that once contained water moisture will evaporate and become voids. These voids are defects that should be minimized in a composite structure, because the higher the void content, the lower the bonding between the composite components. This will lead to a lower mechanical performance as proved by many studies [26,27]. Synthetic epoxy is known to has hydrophobic attribute and jatropha bio-epoxy which consisted of fatty acids is naturally hydrophobic as well, this is the reason that water moisture contents were very low in both specimens.
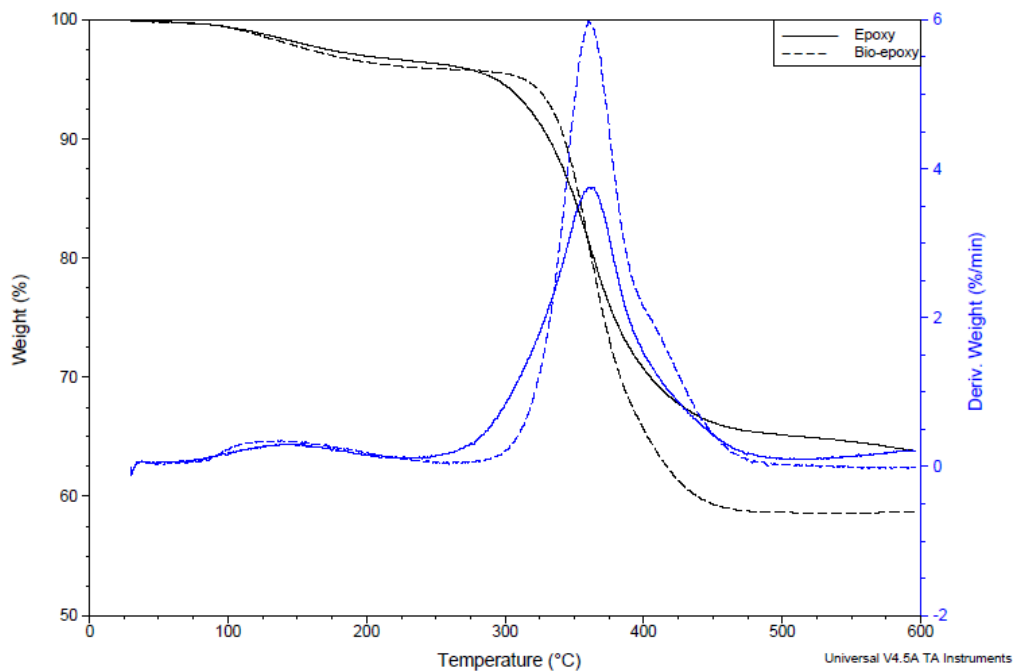
Figure 2. Thermogram of epoxy and jatropha bio-epoxy in a nitrogen atmosphere and derivative weight loss curvature.

Table 3. Thermal stability data of epoxy and bio-epoxy.

Specimens	T_{onset} (°C)	T_{d5} (°C)	T_{d30} (°C)	Heat-Resistant Index (T_s)	Char Temp (°C)	Residual Weight (%)
Epoxy	112	300	405	210	512	64
18 wt.% Bio-epoxy	112	320	380	193	500	59

The second step of thermal degradation occurred at around 96% at 288 °C for both the synthetic epoxy and the blended jatropha bio-epoxy specimens. However, the blended jatropha bio-epoxy specimen lost its weight slightly faster than the synthetic epoxy. This indicated that between room temperature and 288 °C, the blended jatropha bio-epoxy was slightly less thermally stable than the synthetic epoxy. However, once the temperature increased and passed 288 °C, it was found that the

blended jatropha bio-epoxy was more thermally stable than the synthetic epoxy, until it reached 365 °C. After this temperature, the thermal degradation of the blended jatropha bio-epoxy continued to shoot down until 500 °C, when it lost around 41% of its total weight compared to the synthetic epoxy which lost only 34%.

It could be seen that when the jatropha bio-epoxy reached a weight loss of 35% compared to the epoxy at 30% at 400 °C, the aromatic rings began their degradation [28]. By the end of the curvature, the epoxy had a better total thermal stability than the jatropha bio-epoxy. The difference in the residual weight after 500 °C for the synthetic epoxy and the bio-epoxy was 5%. The degradation rate of the blended jatropha bio-epoxy was higher than the synthetic epoxy. Between the temperatures of 245 °C and 475 °C, the weight derivative curvature in Figure 2 revealed a narrower and higher peak for the blended jatropha bio-epoxy compared to a broader and lower peak for the epoxy.

The statistic heat-resistance index (T_s) is a characteristic of the thermal stability of the cured resin. This value was determined from the temperature at 5% weight loss (T_{d5}) and 30% weight loss (T_{d30}) of the specimens obtained from the TGA. The statistic heat-resistant index temperature is calculated from Equation (1) [29–31]. The heat-resistance index is the temperature of the polymer in the physical heat tolerance limit. The temperature of degradation at 30% T_{d30} is important because most of the composite structure consists of 40–70% of reinforcement and 40–60% of resin depending on the fabrication process. In the present study, both specimens, consisting of 53% and 58% of resin epoxy and bio-epoxy respectively, lost 30% of their weight meaning that more than half of the resin's constituent was not there to function as the reinforcement's binder.

$$T_s = 0.49[T_{d5} + 0.6(T_{d30} - T_{d5})] \qquad (1)$$

The value of T_s for the blended jatropha bio-epoxy was 193 °C and 8% lower than the synthetic epoxy which was 210 °C. The blended bio-epoxy had a lower index due to its fatty acid possessing few aliphatic rings, which would weaken the thermal stability [28]. However, both these index values are considered as medium range index values. The specimens exhibited good flame resistance as both were cured with amine, and possessed a good amount of aromatic groups [32,33].

The first weight loss happened at around 300 °C for both specimens. By blending with jatropha bio-epoxy, it was found that below 350 °C it degraded less than the synthetic epoxy. However, the residual weight revealed a decrement of 5% in total thermal stability. Both showed the same region of maximum weight lost, which is around 300–450 °C.

3.2.2. Temperature Transition by DSC

The results of DSC can be seen in the thermograms in Figure 3 and are tabulated in Table 4. It was to determine the thermal behavior of the composite with the blended jatropha bio-epoxy. This thermogram is exothermic as the sensor captured the heat released by the specimens and it is endothermic when the heat is absorbed.

Table 4. Thermal Property for epoxy and bio-epoxy.

Specimens	T_g Onset (°C)	T_{d5} Decomposition (°C)
Epoxy	60	310
18 wt.% Bio-epoxy	62	312

By comparison, the thermograms were similar in curvature but the heat released from the composites with the blended jatropha bio-epoxy was higher than for the fully synthetic composites. The first drop of curvature was at around 55 °C and was the same for both specimens. This drop was endothermic, exhibiting the glass transition temperature as the starting point for the energy required to change the molecular structure inside the epoxy and the jatropha bio-epoxy from a low-energy state to a higher energy state. This reaction changed the state of the epoxy and the jatropha bio-epoxy

from a solid state to a rubbery state. The thermal decomposition continued to happen until around a temperature of 180 °C, it was observed to be another endothermic reaction for both specimens. This is believed to be due to the beginning of the decomposition phase for the epoxy and the bio-epoxy.
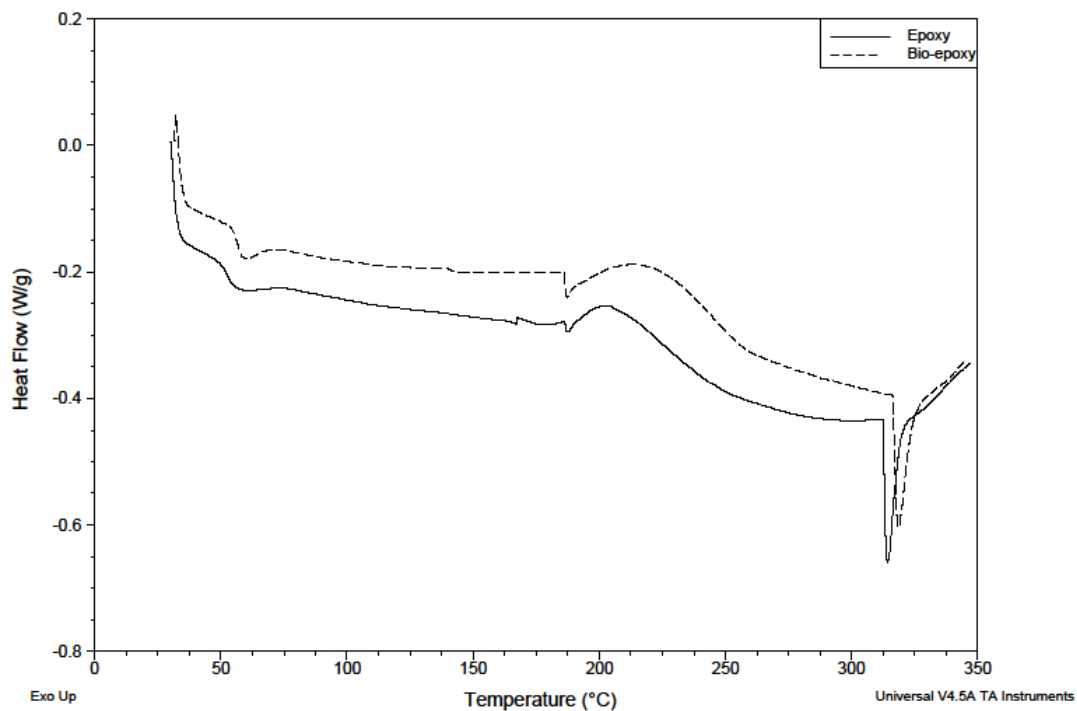
Figure 3. Thermal transitions differential scanning calorimetry (DSC) of the jatropha blended bio-epoxy vs. the synthetic epoxy.

Right after the second endothermic reaction, there was seen to be a very high peak in the exothermic curve for both specimens. This peak was 208 °C for the epoxy and 225 °C for the jatropha bio-epoxy. This was due to the heating process, which might start to change the molecular structure inside the epoxy and the bio-epoxy. This can be verified with a thermogram from the TGA analysis in Figure 2; as the temperature reached 350 °C, both the epoxy and the bio-epoxy began to lose weight rapidly. This indicated that the epoxy and the bio-epoxy started to decompose into the environment because the epoxy and the bio-epoxy were thermoset which has no melting phase.

3.3. Dynamic Mechanical Analysis Results

DMA revealed viscoelastic properties such as the glass transition temperature, the crosslink density, and the temperature dependence of the storage modulus, the loss modulus, and the tan delta of the epoxy and the jatropha bio-epoxy [2]. The graphs of the DMA test are shown in Figure 4 for Tan Delta, Figure 5 for Storage Modulus, and Figure 6 for Loss Modulus. The glass transition temperature can also be determined from the DMA results using three different methods: the onset of the storage modulus drop ($T_{g\,SM}$), the peak of the maximum of the loss modulus ($T_{g\,LM}$), and the peak maximum of tan delta ($T_{g\,TD}$). Table 5 lists the T_g values of the epoxy and the jatropha bio-epoxy obtained from these methods.

Table 5. Transition glass temperature for the epoxy and the jatropha bio-epoxy from the DMA results.

Specimens	$T_{g\,SM}$ from the Storage Modulus Onset Drop (°C)	$T_{g\,LM}$ from the Loss Modulus Maximum Peak (°C)	$T_{g\,TD}$ from the Tan Delta Maximum Peak (°C)
Epoxy	73	75	80
18 wt.% Bio-epoxy	68	70	75
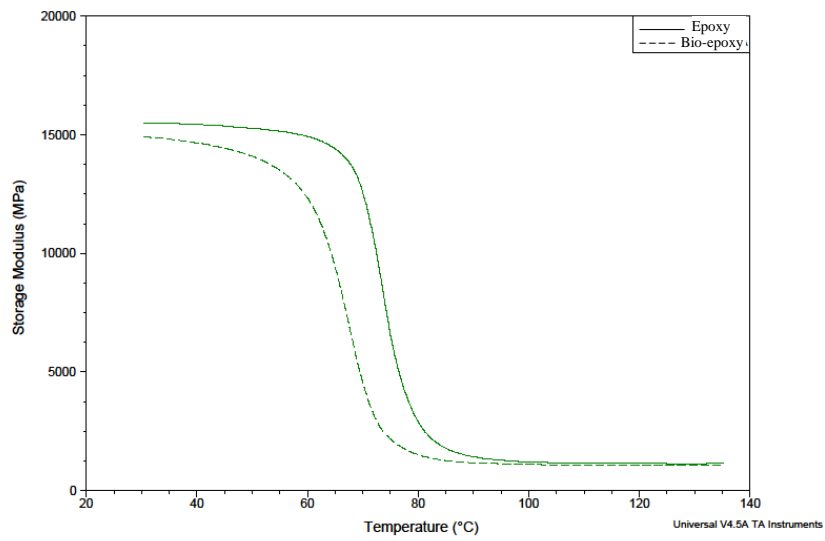
Figure 4. Storage Modulus of the blended jatropha bio-epoxy vs. the synthetic epoxy.
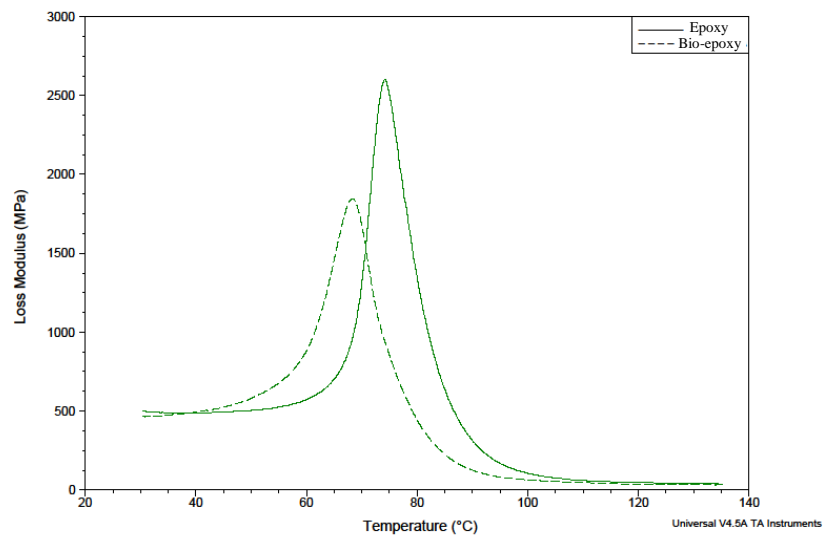
Figure 5. Loss Modulus of the blended jatropha bio-epoxy vs. the synthetic epoxy.
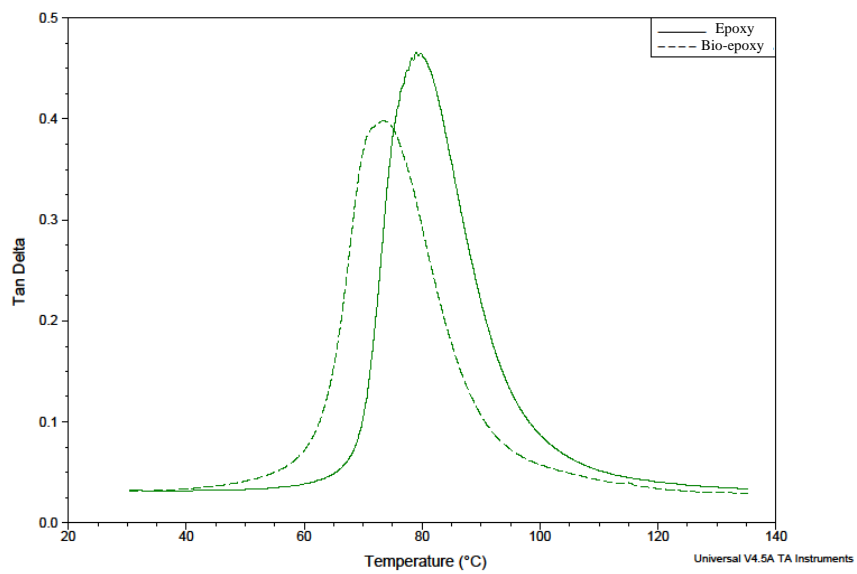
Figure 6. Tan Delta of blended Jatropha bio-epoxy vs. synthetic epoxy.

3.3.1. Storage Modulus

The storage modulus in the viscoelastic polymer represents the elastic portion or the solid-like behavior of the material. In Figure 4, the storage modulus can be divided into three regions: the glassy state, the glass transition region, and the rubbery state. In the glassy state, as the specimens were heated, the storage modulus value decreased, indicating that there was more movement in the polymer network. Looking at the shape of curves, the specimen with the blended jatropha bio-epoxy experienced a higher decrease rate in the storage modulus values than the specimen with the synthetic epoxy. The specimen with the blended jatropha bio-epoxy also had a shorter temperature range for its glassy state. The temperature at the onset of the rapid decrease in the storage modulus was the transition glass temperature $T_{g\,SM}$; the values for these were 73 °C and 68 °C for the epoxy and the bio-epoxy, respectively. The T_g of the jatropha bio-epoxy was lower by 5 °C compared to the epoxy.

3.3.2. Loss Modulus

The loss modulus in the viscoelastic polymer represents the viscous portion or liquid-like behavior of the thermosets. As a polymer becomes more viscous, it will begin to lose its loss modulus capability. Figure 5 shows the loss modulus curve in function of temperature. For the specimen with the blended jatropha bio-epoxy, the loss modulus started to increase significantly as soon as the specimen was heated compared to the specimen with the synthetic epoxy. Furthermore, the width of the peak curve from the specimen with the blended bio-epoxy base line was slightly broader but clearly lower than that of the specimen with the synthetic epoxy. From the maximum peak of the loss modulus curve, $T_{g\,LM}$ was 75 °C and 70 °C for the epoxy and the jatropha bio-epoxy, respectively. They differed by around 5 °C.

3.3.3. Tan Delta δ

The ratio of loss modulus over storage modulus is the tan delta as in Figure 6. The peak maximum of the tan delta curvature was the transition glass temperature according to tan delta $T_{g\,TD}$ of a polymer. The highest $T_{g\,TD}$ was 80 °C and 75 °C for the epoxy and the jatropha bio-epoxy respectively. The T_g of the jatropha bio-epoxy was 5 °C less than the epoxy. In addition, the width of the tan delta peak curvature might suggest the degree of homogeneity of the network. Paramarta et al. and Pan et al. also found the same pattern for bio-based thermosets, whereby a broader peak and a narrower peak was due to a higher catalyst amount in the blended polymer [2,34].

The broader peak of tan delta means less homogeneity [35]. Increasing the fiber/resin interfacial bonding resulted in a reduction in the damping ability since the mobility of the molecular chains at the fiber/resin interface was decreased. A lower energy loss E″ leads to a higher tan delta δ. The damping factor is related to the molecular movements and viscoelasticity properties of the material. In addition, certain defects can contribute towards damping, such as crystal dislocations, grain boundaries, phase boundaries and molecule's interface. The peak of tan delta is commonly identified as the T_g of a polymer ($T_{g\,TD}$). The highest peak $T_{g\,TD}$ for the tan delta curves in Figure 6 is around 80 °C for the synthetic epoxy and 75 °C for the jatropha bio-epoxy. The breadth of the peak exhibits the degree of homogeneity of the polymer network. The sample of the jatropha bio-epoxy has a broader peak at 80 °C compared to 60 °C for the synthetic epoxy. By all these three methods, all the T_g of the bio-epoxy were concluded to be 5 °C less compared to the epoxy.

3.4. Flammability Result

The results of the flammability test are shown in Table 6. Most of the time, bio-based composites are considered for low loading or non-load-bearing loading and for almost no critical loading conditions such as secondary structures, insulating panels, interior panels, under sit floor panels for aircraft application, mechanical and civil structures. This is one of the reasons why the flammability test was necessary.

Table 6. Flammability characteristics of the epoxy and the jatropha bio-epoxy.

Composite Structure	Thickness (mm)	Average Time to Self-Extinguished (s)	Burning Rate in HB	Dripping Occurred
0 wt.% bio-epoxy	2.24	29.3	Yes	No
18 wt.% bio-epoxy	2.42	66.7	Yes	No

Normally, most bio-based composites are less fire resistant compared to synthetic ones and as expected, the horizontal flammability test showed that blended jatropha bio-epoxy has lower fire resistance. The times for the flame to be self-extinguished are double for the blended bio-epoxy, which were 66.7 s and 29.3 s for the jatropha bio-epoxy and the epoxy, respectively. This is believed to be due to the less aromatic group occurring in the bio-epoxy as can be inspected from the FT-IR/ATR spectrum obtained in Figure 1. No dripping occurred during the fire, and the flame propagation was very slow and comparable for both the jatropha bio-epoxy and the epoxy.

4. Conclusions

The carbon fiber/jatropha bio-epoxy and the carbon fiber/epoxy laminate composite structures were fabricated using the vacuum infusion method and were subjected to thermal testing such as TGA, DSC, and DMA analysis, FTIR analysis, and flammability testing. Based on the results, by adding 18 wt.% of the jatropha bio-epoxy into the composite structure matrix, the following conclusions are drawn:

- Chemical bonding of cured blended jatropha bio-epoxy and synthetic epoxy are almost identical.
- The blended jatropha bio-epoxy composite structure has better thermal stability and thermal degradation in the range 288–350 °C.
- Amongst the methods for finding the glass transition temperature, T_g, of this blended jatropha bio-epoxy composite structure, the highest T_g temperature was obtained by the tan delta curve, which is 75 °C. All the curves from DMA, TGA, and DSC analyses indicate that the jatropha bio-epoxy blended well into the matrix as only one T_g occurs for each curve.
- During temperature increase, the blended jatropha bio-epoxy composite structure started to lose its stiffness and damping ability earlier than the composite structure with the fully synthetic epoxy.
- In terms of flammability, the self-extinguishing capability was established at 66.7 s after propagation of a small flame.
- Some interesting comparison characteristics between them are tabulated in Table 7.

Table 7. Flammability characteristics of the epoxy and the jatropha bio-epoxy.

	Composite with Fully Synthetic Epoxy	Composite with 18 wt.% Blended Jatropha Bio-Epoxy
Heat-resistant Index T_s (°C)	210.0	193.0
Glass Transition T_g (°C)		
Maximum temperature	80.0	75.0
Minimum temperature	73.0	68.0
Time to self-extinguished (s)	29.3	66.7

References

1. Caillol, S.; David, G.; Boutevin, B.; Pascault, J.; de Lyon, U. Biobased Thermosetting Epoxy: Present and Future. *Chem. Rev.* **2014**, *114*, 1082–1115. [CrossRef]

2. Paramarta, A.; Webster, D.C. Bio-based high performance epoxy-anhydride thermosets for structural composites: The effect of composition variables. *React. Funct. Polym.* **2016**, *105*, 140–149. [CrossRef]

3. Hafiezal, M.R.M.; Abdan, K.; Azaman, M.D.; Abidin, Z.Z.; Hanafee, Z.M. Initial Study of New Bio-based Epoxy in Carbon Fiber Reinforced Composite Panel Manufactured by Vacuum Assisted Resin Transfer Moulding. *AIP Conf. Proc.* **2017**, 1885. [CrossRef]

4. Hafiezal, M.R.M.; Abdan, K.; Abidin, Z.Z.; Azaman, M.D.; Hanafee, Z.M. Physical Characterization of Carbon Fiber Reinforced Composite with Blended Epoxidized Jatropha Oil (EJO). *IOP Conf. Ser. Mater. Sci. Eng.* **2018**, 368. [CrossRef]

5. Min, M.; Yaakob, Z.; Kamarudin, S.; Chuah, L. Synthesis and characterization of Jatropha (*Jatropha curcas* L) oil-based polyurethane wood adhesive. *Ind. Crop. Prod.* **2014**, *60*, 177–185.

6. Sammaiah, A.; Padmaja, K.V.; Badari, R.; Prasad, N. Synthesis of Epoxy Jatropha Oil and its Evaluation for Lubricant Properties. *J. Eleo Sci.* **2014**, *643*, 637–643. [CrossRef]

7. Ng, E.N.S. Characteristics and Composition of Jatropha curcas Oils, Variety Congo-Brazzaville. *Res. J. Appl. Sci. Eng. Technol.* **2009**, *1*, 154–159.

8. Kumar, M.N.S.; Yaakob, Z.; Mohan, N.; Babu, S.P.K. Mechanical and Abrasive Wear Studies on Biobased Jatropha Oil Cake Incorporated Glass—Epoxy Composites. *J. Am. Oil Chem. Soc.* **2010**, *87*, 929–936. [CrossRef]

9. Niedermann, P.; Szebényi, G.; Toldy, A. Characterization of high glass transition temperature sugar-based epoxy resin composites with jute and carbon fibre reinforcement. *Compos. Sci. Technol.* **2015**, *117*, 62–68. [CrossRef]

10. Liu, K.; Madbouly, S.A.; Kessler, M.R. Biorenewable thermosetting copolymer based on soybean oil and eugenol. *Eur. Polym. J.* **2015**, *69*, 16–28. [CrossRef]

11. Gogoi, P.; Boruah, M.; Sharma, S.; Dolui, S.K. Blends of epoxidized alkyd resins based on jatropha oil and the epoxidized oil cured with aqueous citric acid solution: A green technology approach. *ACS Sustain. Chem. Eng.* **2015**, *3*, 261–268. [CrossRef]

12. Gogoi, P.; Boruah, M.; Bora, C.; Dolui, S.K. Jatropha curcas oil based alkyd/epoxy resin/expanded graphite (EG) reinforced bio-composite: Evaluation of the thermal, mechanical and flame retardancy properties. *Prog. Org. Coat.* **2014**, *77*, 87–93. [CrossRef]

13. Szolnoki, B.; Bocz, K.; Marosi, G.; Toldy, A. Flame Retardancy of Sorbitol Based Bioepoxy via Combined Solid and Gas Phase Action. *Polymers* **2016**, *8*, 322. [CrossRef]

14. Ezzah, F. Production Characterization and Kinetic Modelling of Malaysia Jatropha Oil Based Bio-Epoxy Resins. Master's Thesis, University Putra Malaysia, Seri Kembangan, Malaysia, 2016.

15. Abdullah, B.M.; Salih, N.; Salimon, J. Optimization of the chemoenzymatic mono-epoxidation of linoleic acid using D-optimal design. *J. Saudi Chem. Soc.* **2014**, *18*, 276–287. [CrossRef]

16. Taylor, P.; Ikhuoria, E.U.; Obuleke, R.O.; Okieimen, F.E. Studies on the Kinetics of Epoxidation of the Methyl Esters of Parkia Biglobosa Seed Oil. *J. Macromol. Sci. Part A Pure Appl. Chem.* **2007**, 37–41. [CrossRef]

17. Hazmi, A.S.A.; Aung, M.M.; Abdullah, L.C.; Salleh, M.Z.; Mahmood, M.H. Producing Jatropha oil-based polyol via epoxidatioin and ring opening. *Ind. Crops. Prod.* **2013**, *50*, 563–567. [CrossRef]

18. Ishak, A.A.; Salimon, J. Synthesis of Rubber Seed Oil and Trimethylolpropane Based Biolubricant Base Stocks. *Malays. J. Anal. Sci.* **2013**, *17*, 414–421.

19. Kadam, A.; Pawar, M.; Yemul, O.; Thamke, V.; Kodam, K. Biodegradable biobased epoxy resin from karanja oil. *Polymer* **2015**, *72*, 82–92. [CrossRef]

20. Manthey, N.W.; Cardona, F.; Aravinthan, T. Cure Kinetic Study of Epoxidized Hemp Oil Cured with a Multiple Catalytic System. *J. Appl. Polym. Sci.* **2011**, *125*, 511–517. [CrossRef]

21. Chauhan, P.S. Epoxidation in karanja oil for biolubricant applications. *Int. J. Pharm. Biol. Sci. Arch.* **2013**, *1*, 61–70.

22. Tomas, V.; Petrovic, Z.S. Optimization of the Chemoenzymatic Epoxidation of Soybean Oil. *J. Am. Oil Chem. Soc.* **2006**, *83*, 247–252.

23. Mincheva, R.; Delangre, A.; Raquez, J.-M.; Narayan, R.; Dubois, P. Biobased Polyesters with Composition-Dependent Thermomechanical Properties: Synthesis and Characterization of Poly(butylene succinate-co-butylene azelate). *Biomacromolecules* **2013**, *14*, 890–899. [CrossRef]

24. Boll, D.J.; Bascom, W.D.; Motiee, B. Moisture Absorption by Structural Epoxy-Matrix Carbon-fiber Composites. *Compos. Sci. Technol.* **1985**, *24*, 253–273. [CrossRef]

25. Gibbins, M.N.; Hoffman, D.J. Environmental Exposure Effects on Composite Materials for Commercial Aircraft. *NASA Contract. Rep.* **1982**, 69–76.

26. Xingxing, W.; Min, L.; Qing, W.; Yizhou, G.; Yanxia, L.; Shaokai, W.; Zuoguang, Z. Influence of Surface State on Moisture Sensitivity of Carbon Fiber and Its Composite Interfacial Properties. *J. Wuhan Univ. Technol. Sci. Ed.* **2016**, 757–764. [CrossRef]

27. Zafar, A.; Bertocco, F.; Rauhe, J.C. Investigation of the long term effects of moisture on carbon fibre and epoxy matrix composites. *Compos. Sci. Technol.* **2012**, *72*, 656–666. [CrossRef]

28. Kuo, P.; de Assis, L.; Sheen, Y.; Sain, M. Thermal degradation of extractive-based bio-epoxy monomer and network: Kinetics and mechanism. *J. Anal. Appl. Pyrolysis.* **2016**, *117*, 199–213. [CrossRef]

29. Lehrle, R.S.; Williams, R.J.; Birmingham, B. Thermal Degradation of Bacterial Poly(hydroxybutyric acid): Mechanisms from the Dependence of Pyrolysis Yields on Sample Thickness. *Macromolecules* **1994**, *27*, 3782–3789. [CrossRef]

30. Bibiao, J.; Jianjun, H.; Wenyun, W.; Luxia, J.; Xinxian, C. Synthesis and properties of novel polybismaleimide oligomers. *Eur. Polym. J.* **2001**, *37*, 463–470. [CrossRef]

31. Chiu, Y.; Chou, I.; Tseng, W.; Ma, C.M. Preparation and thermal properties of diglycidylether sulfone epoxy. *Polym. Degrad. Stab.* **2008**, *93*, 668–676. [CrossRef]

32. Plastic Heat Resistance Index and Classification. Available online: http://www.sztengye-vacuumforming.com/news/plastic-heat-resistance-index-and-classificati-4452617.html (accessed on 1 June 2018).

33. Paluvai, N.R.; Mohanty, S.; Nayak, S.K. Synthesis and Modifications of Epoxy Resins and Their Composites: A Review. *Polym. Plast. Technol. Eng.* **2014**, *53*, 1723–1758. [CrossRef]

34. Pan, X.; Sengupta, P.; Webster, D.C. High Biobased Content Epoxy À Anhydride Thermosets from Epoxidized Sucrose Esters of Fatty Acids. *Biomacromolecules* **2011**, *12*, 2416–2428. [CrossRef] [PubMed]

35. Campanella, A.; Zhan, M.; Watt, P.; Grous, A.T.; Shen, C.; Wool, R.P. Triglyceride-based thermosetting resins with different reactive diluents and fiber reinforced composite applications. *Compos. Part A* **2015**, *72*, 192–199. [CrossRef]